

NACA RM No. L8K04

RM L8K04

0143873

TECH LIBRARY KAFB, NM

~~CONFIDENTIAL~~  
NACA

## RESEARCH MEMORANDUM

LANGLEY FREE-FLIGHT-TUNNEL INVESTIGATION OF THE AUTOMATIC  
LATERAL STABILITY CHARACTERISTICS OF A MODEL EQUIPPED  
WITH A GYRO STABILIZING UNIT THAT PROVIDED EITHER  
FLICKER-TYPE OR HUNTING CONTROL

By

Robert O. Schade

Langley Aeronautical Laboratory  
Langley Field, Va.

## CLASSIFIED DOCUMENT

This document contains classified information and is exempt from automatic declassification under Executive Order 11652, National Defense of the United States, and the Espionage Act, USC 50. Its transmission or the revelation of its contents in any manner to an unauthorized person is prohibited by law. Information so classified shall be imparted only to persons in the military and naval services of the United States, to appropriate civilian officers and employees of the Federal Government who have a legitimate need therefor, and to United States citizens, in loyalty and discretion who of necessity must be informed thereof.

NATIONAL ADVISORY COMMITTEE  
FOR AERONAUTICS

WASHINGTON  
January 11, 1949

~~CONFIDENTIAL~~

7153

159913

Classification cancelled (or changed to) Unclassified  
By Auth: NASA Tech Pub Announcement 7551  
(OFFICE AUTHORIZED TO CHANGE)

By 23 Dec 63  
AK

GRADE OF OFFICER (MAKING CHANGE)  
11 Apr 61  
DATE



## NATIONAL ADVISORY COMMITTEE FOR AERONAUTICS

## RESEARCH MEMORANDUM

LANGLEY FREE-FLIGHT-TUNNEL INVESTIGATION OF THE AUTOMATIC  
LATERAL STABILITY CHARACTERISTICS OF A MODEL EQUIPPED  
WITH A GYRO STABILIZING UNIT THAT PROVIDED EITHER  
FLICKER-TYPE OR HUNTING CONTROL

By Robert O. Schade

## SUMMARY

An investigation was undertaken in the Langley free-flight tunnel to determine the automatic lateral stability characteristics of a model equipped with a gyro stabilizing unit that gave response to bank and yaw. Flight tests of the model were made with a flicker-type (full-on or full-off) control system and with this system modified by the addition of an attachment that produced a hunting control which resulted in an effectively proportional response to bank and yaw. The effects of varying the cant angle and rudder deflections were investigated. The tilt angle of the gyroscope was held constant for all tests.

Stable flights were obtained with the flicker-type automatic control, and the amplitude of the oscillations was decreased by adding the attachment which provided hunting control. Varying the cant angle between  $22.5^\circ$  and  $90^\circ$  had no pronounced effect on the stability except near  $90^\circ$  where the flight characteristics became poor. There was no pronounced effect on the stability by reducing the rudder deflection from  $\pm 7^\circ$  to  $0^\circ$ . Comparison of computed and measured rolling motions obtained with flicker automatic control showed good agreement.

In connection with this investigation a systematic calibration was made of the gyro unit to determine its response to angles of yaw and bank for various angles of cant and tilt, and formulas were developed for calculating the response of the gyroscope. The experimental and calculated results were found to be in good agreement.

## INTRODUCTION

An investigation to determine the automatic lateral stability characteristics of a model equipped with a gyro stabilizing unit that gave response to yaw and bank has been made in the Langley free-flight tunnel.

Flight tests of the model were made with a flicker-type (full-on or full-off) control system and with this system modified by the addition of an attachment that produced hunting control which resulted in an effectively proportional response to bank and yaw. The tilt angle of the gyroscope was held constant for all tests, and the effect of varying the response to yaw and bank was studied by changing the cant angle. The effect of varying the rudder deflection was also investigated. Correlation of calculated and experimental rolling motions was made for the model with flicker automatic control only.

Presented in an appendix are the results of a systematic calibration made on the gyro unit to determine its response to angles of yaw and bank for various angles of cant and tilt and formulas that were developed for calculating the response of the gyroscope. A comparison is made between the experimental and calculated response. An example illustrating the use of some of the formulas is also shown.

#### SYMBOLS

$\phi$	angle of bank, degrees
$\beta$	angle of sideslip, degrees
$\psi$	angle of yaw, degrees
$C$	cant angle (angle between inner and outer gimbals, positive direction shown in fig. 1), degrees
$T$	tilt angle (angle between outer gimbal and line of flight, positive direction shown in fig. 1), degrees
$\tau$	response or rotation of pick-off (rotation of outer gimbal about roll axis with respect to case, positive rotation is counterclockwise as viewed from rear), degrees
$\theta$	transition angle, (angle to which pick-off drum is moved by reversing attachment; or the angle of pick-off contact below which hunting control occurs and above which the control becomes held full on), degrees
$\delta_a$	aileron deflection, degrees
$\delta_r$	rudder deflection, degrees
$C_{n\beta}$	rate of change of yawing-moment coefficient with angle of sideslip, per degree $\left(\frac{\partial C_n}{\partial \beta}\right)$

$C_{l\beta}$	rate of change of rolling-moment coefficient with angle of sideslip, per degree $\left(\frac{\partial C_l}{\partial \beta}\right)$
$C_{Y\beta}$	rate of change of lateral-force coefficient with angle of sideslip, per degree $\left(\frac{\partial C_Y}{\partial \beta}\right)$
t	time, seconds
m	mass
$\rho$	mass density of air, slugs per cubic foot
S	wing area, square feet
b	span, feet

## APPARATUS AND METHODS

### Tunnel and Model

The investigation was conducted in the Langley free-flight tunnel, which is designed for the flight-testing of unrestrained, dynamic models. A complete description of the tunnel and its operation is presented in reference 1. A photograph of the test model flying in the tunnel is presented in figure 2.

The model used in the tests was approximately a  $\frac{1}{3}$ -scale model of the Navy Design No. 13ADR (Gargoyle) pilotless aircraft except that the airfoil section of the model was a modified Rhode St. Genese 35 which is an airfoil that gives a value of maximum lift at low scale nearly equal to that of a full-scale airplane. The mass characteristics of the model, however, were not scaled down from the Gargoyle inasmuch as the low air-speed of the tunnel limited the wing loading of the model to a relatively low value. The aerodynamic and mass characteristics are presented in table I for the full-scale aircraft that is represented by the model. Photographs of the model are presented in figure 3 and a sketch of the model is shown in figure 4.

### Gyro Unit

The gyroscope used in the investigation had two degrees of gimbal freedom, one about the X-axis and one about the Y-axis. An effective third degree of gimbal freedom about the Z-axis was achieved by a

combination of movements about the X- and Y-axes so that the attitude of the spin axis of the gyroscope could remain fixed in space. The gyro motor had a counterclockwise rotation, looking down from the top at  $0^\circ$  tilt and  $90^\circ$  cant, and a constant speed of 10,000 rpm.

A cut-away drawing showing the details of the gyro unit is presented in figure 5. The reversing attachment used for hunting control and the pilot's override solenoid mechanism are shown mounted at the rear of the case. A portion of a gear attached to the inside gimbal was used to cage the gyroscope at predetermined cant angles. The pick-off drum and pick-off contact shown in figure 5 are attached to the case and outside gimbal, respectively.

By a slight variation of the mechanical attachments of the gyro pilot, automatic flicker-type and hunting control were obtained. For the discussion of the two types of automatic controls it is assumed that the gyro is set at a cant angle of  $90^\circ$  and a tilt angle of  $0^\circ$  which gives response only to angle of bank. The response of the controls to pick-off contact rotation is the same whether the pick-off rotation is obtained from angles of yaw or bank.

The pilot's override control is obtained by energizing the override solenoid (fig. 5) which in turn rotates the pick-off drum to give corrective control. If the automatic control proved to be destabilizing or the model was drifting into a tunnel wall the pilot was able to override it and prevent a crash.

Flicker-type control.- For the flicker control, the reversing attachment (fig. 5, item 2) is removed and the operation is as follows: If a disturbance in bank to the right is assumed, the pick-off drum (fig. 5, item 5) rotates to the right since it is attached to the gyro case and therefore to the model. The attitude of the pick-off contact (fig. 5, item 7) tends to remain fixed in space since it is mounted on the outside gimbal. Thus there is a relative movement of the pick-off contact on the pick-off drum that closes an electrical circuit (fig. 5, item 8) through the left segment of the pick-off drum to one side of the control actuating mechanism (fig. 5, item 3) which moves the left controls to full deflection to return the model to zero bank. This type of control will remain full on until zero bank is obtained, causing the model to overshoot its zero position. With zero time lag the process will be repeated but in the opposite direction as soon as the model passes zero bank.

Hunting-type control.- For the hunting control the reversing attachment is connected to the control actuating mechanism as shown in figure 5. The screws for varying the transition angle  $\theta$  are shown on the reversing attachment.

The operation of this type of control is as follows: If the angle of bank is assumed to be to the right, there is a relative movement of the

pick-off contact to the left on the pick-off drum. This closes an electrical circuit from the left segment of the pick-off drum to one side of the control actuating mechanism. When this mechanism is energized the left controls operate to return the model to zero bank and the reversing attachment rotates the pick-off drum to the left to its preset transition angle. For the case where the transition angle is larger than the angle of bank, the pick-off contact will now be on the right side of the pick-off drum, causing the electrical circuit to operate the opposite side of the control actuating mechanisms thereby changing the controls from left to right and the pick-off drum from left to right. This reversing of the controls will cause a hunting motion that continues as long as the transition angle is larger than the angle of bank. This hunting control is effectively proportional since averaging the control motions will produce a resultant control-position curve that is approximately proportional to angle of bank. For the case where the transition angle is less than the angle of bank, the pick-off contact is still on the left side of the pick-off drum when the pick-off drum is rotated by the reversing attachment and will not make contact on the opposite or right segment until the angle of bank decreases to less than the transition angle. This system therefore gives effectively flicker control when the angle of bank or pick-off contact rotation is greater than the transition angle and proportional control when the angle of bank or pick-off contact rotation is less than the transition angle.

Forced-oscillation tests.— Results of forced-oscillation calibrations made on an oscillating table to determine the automatic control characteristics are shown in figures 6 to 8. The right aileron control positions were read by means of a control-position recorder while the model was banked at 2.75 cycles per second. These oscillating-table tests did not necessarily simulate any specific flight condition but were made to show the response of the gyroscope in terms of control position with angle of bank for each of the two types of automatic control. For these tests the maximum aileron deflection was  $\pm 25^\circ$ .

#### Calculations

Calculations were made by a simple graphical method similar to that shown in figure 1 of reference 2 to determine the rolling motion of the model with a flicker-type automatic pilot assuming no yaw caused by ailerons or rolling and a time lag of 0.03 second. The calculated results were correlated with those obtained from flight tests.

Some calculations were attempted for the hunting control using variations of the method of reference 2 but the results did not appear to be reliable and the development of the new method for making these calculations was considered beyond the scope of this investigation.

## TESTS

Flight tests were made with both flicker and hunting control. The effects of varying cant angle and rudder deflection were studied in the flights with hunting control. The values of the different parameters varied in the course of the tests are given in table II. All flight tests were made at a lift coefficient of approximately 0.95 which corresponded to an angle of attack of  $13.5^\circ$  and to a tilt angle of  $-13.5^\circ$  since the longitudinal axis of the gyroscope was mounted parallel to the longitudinal axis of the airplane. In the tests where the ailerons and rudders were used for lateral control they were linked together electrically so that their operation was simultaneous. Motion-picture records of the lateral motions of the model were made for each of the conditions.

## RESULTS AND DISCUSSION

Results of forced-oscillation tests are shown in figures 6 to 8. Figure 6 shows that the flicker control had a lag (time between signal and maximum control deflection) of approximately 0.03 second. The jagged portion of the aileron-control-position curve as maximum deflection was first reached was caused by the rebounding of the controls off the stop. Figures 7 and 8 illustrate two variations of the hunting control obtained by varying the transition angle. The frequency of the controls can be seen to be approximately 16 cycles per second for the continuous hunting control (fig. 7) but is of course equal to the frequency of the rolling motion for the flicker-type control (fig. 6).

Records of flight tests are presented in figures 9 to 13 as plots of displacement of the model in bank and yaw against time. The flight records are not completely steady even in the most stable conditions because the model in flight is subjected to a continual series of disturbances caused by the relatively gusty air in the tunnel. Notation of manual-control operation during tests is shown in the flight-test figures.

It can be seen from the flight records that for most flights the model was out of trim to the right (+) in bank and to the left (-) in yaw and was therefore flying in a steady sideslip. It is believed that the results of the flight tests with regard to automatic stability were not appreciably affected by this asymmetry.

## Effect of Type of Control

Records of flights in which the type of control was varied are presented in figure 9. It can be seen that stable flights were possible with all types of automatic control but that with flicker control, which



has a constant amplitude oscillation, the model banked considerably more than with hunting control. The increased steadiness of the model with hunting control was caused by the effectively proportional response at angles of bank and yaw less than the transition angle which reduced the average control deflection as the angle of bank was reduced and therefore minimized the overshooting. Varying the hunting control by changing the transition angle from  $10^\circ$  to  $5^\circ$  (which therefore causes the flicker control to operate at smaller angles of pick-off rotation) appeared to cause a slight increase in frequency and decrease in amplitude of the oscillations.

Although in these low-speed flights the flicker-type control appeared to be satisfactory, in full-scale tests where the airspeed is considerably higher, the shorter periods combined with time lag will cause the phase lag to be more critical and this type of control might have characteristics that prohibit its use.

#### Effect of Cant Angle

The effect of varying the cant angle on the flight characteristics of the model is shown in figure 10. The variation of the cant angle from  $45^\circ$  to  $22.5^\circ$  had no pronounced effect on the amplitude or frequency of the oscillations in flight; but when the cant angle was increased from  $45^\circ$  to  $90^\circ$ , poor flight characteristics were noted. In this  $90^\circ$  cant condition with  $-13.5^\circ$  tilt the model yawed and banked excessively because of reversed response to yaw, and frequent manual override control was required to prevent the model from crashing. The rather low value of  $C_{n_p}$  for this model, as shown in table I, probably aggravated this condition in that the model had no strong tendency to weathercock. The reversed response obtained from the gyroscope with a cant angle of  $90^\circ$  is shown by a relationship in the appendix under the discussion of formula (1). This relationship shows that for positive response the tilt angle must be between  $\pm 90^\circ$  and the cant angle must be greater than zero and less than  $(90^\circ + \text{tilt})$ . In this condition where the cant angle is  $90^\circ$  and the tilt angle is  $-13.5^\circ$  the requirements for positive response will not be met, since the cant angle will not be less than  $(90^\circ + \text{tilt})$ . Either decreasing the cant angle from  $90^\circ$  or increasing the tilt angle in the positive direction would tend to eliminate this reversal effect. No flights were attempted below a cant angle of  $22.5^\circ$  since a gust or elevator movement resulting in a change in angle of attack in the positive direction would be likely to cause the cant angle to approach zero and result in the gyroscope tumbling.

#### Effect of Rudder Operation

The effect of rudder operation on the flight characteristics of the model is shown in figure 11. A rudder deflection of  $\pm 7^\circ$  was used in most

of the tests. This deflection was found from manually controlled flights to be the value which minimized the adverse yawing caused by ailerons and rolling velocity. With the rudder inoperative, there was a slight increase in the amplitude of the oscillations which was probably caused by the adverse yawing moments.

### Effect of Control Neutralizing Springs

Flight-test records showing the effect on roll stabilization of removing the control neutralizing springs used on the control actuating mechanism (fig. 5, item 3) are presented in figure 12. The results show that there was no noticeable difference in flight characteristics when the control neutralizing springs were removed.

### Comparison of Calculated and Experimental Results

A comparison of the rolling motions and those obtained from flight records of the model with flicker automatic control are presented in figure 13. The agreement is considered good since the calculated results indicate an amplitude of  $14.0^\circ$  and a period of 0.30 second compared to an average measured amplitude of  $13.2^\circ$  and a period of 0.33 second.

### CONCLUSIONS

The following conclusions were drawn from an investigation in the Langley free-flight tunnel of the automatic lateral stability characteristics of a model equipped with a gyro stabilizing unit that gave response to bank and yaw:

1. Stable flights were obtained with a flicker-type automatic control, which gave constant amplitude oscillations.
2. The amplitude of the oscillations was decreased by adding an attachment which provided a hunting control that gave effectively proportional response when the pick-off rotation was less than the transition angle and flicker control when the pick-off rotation was greater than the transition angle.
3. Varying the cant angle between  $22.5^\circ$  and  $90^\circ$  had no pronounced effect on the stability except near  $90^\circ$  where reversed response to angles of yaw caused poor flight characteristics.
4. There was no pronounced effect on the stability of reducing rudder deflection from  $\pm 7^\circ$  to  $0^\circ$ .

5. Comparison of computed and measured rolling motions obtained with flicker automatic control showed good agreement.

Langley Aeronautical Laboratory  
National Advisory Committee for Aeronautics  
Langley Field, Va.

## APPENDIX

## GYRO RESPONSE TO YAW AND BANK FOR VARIOUS

## ANGLES OF CANT AND TILT

## INTRODUCTION

In connection with the investigation conducted in the Langley free-flight tunnel on a model equipped with a gyro unit to give automatic lateral stability, a systematic calibration was made of the gyroscope in which its response to angles of yaw and bank with various angles of cant and tilt was determined. Formulas were also developed from which the response of the gyroscope could be determined. These results are of general interest in connection with aircraft having gyro stabilization and should be useful in determining the automatic stability of guided missiles which, during a single flight, have large variations in flight path or angle of attack which result in large changes in cant or tilt angle.

The formulas and their correlation with the gyro calibration are discussed herein.

## ANALYSIS

With the assumption that this gyroscope, like a free gyroscope, tends to remain fixed in space, a set of geometric formulas was derived, using equation (16) of reference 3, for calculating the response of the gyroscope to yaw for various angles of cant and tilt. The solution of these formulas gave the angle between two planes or the pick-off rotation  $\tau$  required to keep the spin axis fixed in space for various changes in cant, tilt, bank, and yaw angles. The relationships used in the derivation of the yaw formula (formula (1)) are presented in figure 14. The plane ABC was determined for the forward portion of the gyroscope by assuming some cant angle and tilt angle which in turn located the gyro spin axis, line AB, and the axis of pick-off rotation, line AC. It was then assumed that plane ABC was rotated through some angle about the Z-axis to plane AB'C' simulating a change in angle of yaw. In order that the now displaced gyro spin axis AB' can return to its original position line AB (which is necessary to keep the gyro spin axis fixed in space) the plane AB'C' will have to rotate about the axis of pick-off rotation to plane AB''C', and the cant angle will have to increase, causing line AB'' to coincide with line AB (original gyro spin axis). The pick-off rotation, or angle between the two planes AB'C' and AB''C', is obtained from a formula in reference 3. In actual operation, the

gyro spin axis, of course, remains fixed in space and the lines AB' and AB'' which show a movement of the gyro spin axis are used only for illustrative purposes and will not actually exist.

The following formula gives the response of the gyroscope to angle of yaw for different angles of tilt and cant:

$$\tau = \pm \cos^{-1} \left[ \frac{A \cos \psi + B}{\sqrt{(D \sin^2 \psi + E \cos^2 \psi + F \cos \psi + G)H}} \right] \quad (1)$$

where

$$\begin{aligned} A &= \sin T \cos T \sin (C - T) \cos (C - T) + \sin^2 T \cos^2 (C - T) \\ B &= \sin T \cos T \sin (C - T) \cos (C - T) + \cos^2 T \sin^2 (C - T) \\ D &= \cos^2 T \\ E &= \cos^2 T \sin^2 (C - T) \\ F &= 2 \sin T \cos T \sin (C - T) \cos (C - T) \\ G &= \sin^2 T \cos^2 (C - T) \\ H &= E + F + G \end{aligned}$$

The response  $\tau$  is positive for positive angles of bank and yaw when  $-90^\circ < T < 90^\circ$  and when  $0 < C < 90^\circ + T$ .

For the case where tilt angle is held constant at  $0^\circ$  and cant angle is varied between  $0^\circ$  and  $90^\circ$ , formula (1) can be simplified to

$$\tau = \sin^{-1} \sqrt{\frac{1}{1 + \frac{\tan^2 C}{\sin^2 \psi}}} \quad (2)$$

Within the above-mentioned conditions of cant and tilt angles the response is positive.

For the case in which the cant angle is held constant at  $90^\circ$  and the tilt angle is varied between  $0^\circ$  to  $90^\circ$  the following simple approximate relationship, which is within about  $\pm 1^\circ$  accuracy up to  $50^\circ$  yaw, can be used

$$\tau = \psi \sin T \quad (3)$$

The formula for the response of the gyro to angles of bank with cant and tilt angle variation is:

$$\tau = \pm \cos^{-1} \left[ \frac{A \cos \phi + B}{\sqrt{(D \sin^2 \phi + E \cos^2 \phi + F \cos \phi + G)H}} \right] \quad (4)$$

where

$$\begin{aligned}
 A &= \sin (T - 90^\circ) \cos (T - 90^\circ) \sin [C - (T - 90^\circ)] \cos [C - (T - 90^\circ)] \\
 &\quad + \sin^2(T - 90^\circ) \cos^2[C - (T - 90^\circ)] \\
 B &= \sin (T - 90^\circ) \cos (T - 90^\circ) \sin [C - (T - 90^\circ)] \cos [C - (T - 90^\circ)] \\
 &\quad + \cos^2(T - 90^\circ) \sin^2[C - (T - 90^\circ)] \\
 D &= \cos^2(T - 90^\circ) \\
 E &= \cos^2(T - 90^\circ) \sin^2[C - (T - 90^\circ)] \\
 F &= 2 \sin (T - 90^\circ) \cos (T - 90^\circ) \sin [C - (T - 90^\circ)] \cos [C - (T - 90^\circ)] \\
 G &= \sin^2(T - 90^\circ) \cos^2[C - (T - 90^\circ)] \\
 H &= E + F + G
 \end{aligned}$$

The response  $\tau$  is positive for positive angles of bank and yaw when  $0^\circ < T < 90^\circ$  and when  $T < C < 180^\circ$ . Positive response may also be obtained when  $-90^\circ < T < 0^\circ$  if  $0^\circ < C < 180^\circ - T$ .

The formula for the response to bank with the cant angle at  $90^\circ$  and a tilt angle variation from  $-90^\circ$  to  $90^\circ$  is:

$$\tau = \phi \cos T \quad (5)$$

The response is positive for these conditions of cant and tilt angles.

In the case where the tilt angle is held constant at  $0^\circ$  there is no change in response to bank over a range of cant angles from  $0^\circ$  to  $90^\circ$  and this simple relationship holds:

$$\tau = \phi \quad (6)$$

#### APPARATUS AND METHODS

For the calibration, the gyro unit was mounted in such a manner that it could be banked and yawed independently. The calibration was made by setting the tilt angle at  $0^\circ$  and determining the response of the gyroscope to bank or yaw for various cant angles and then by setting the cant angle at  $90^\circ$  and determining the response for various tilt angles.

The calibration included tests to determine variations in response or pick-off rotation over a range of cant angles from  $11.25^\circ$  to  $90^\circ$  in  $11.25^\circ$  increments. This particular variation was used since the cant-angle setting was achieved by a gear which had 16 teeth in  $90^\circ$ . (See fig. 5.) No calibration was made at a cant angle of  $0^\circ$  since this is an unstable position for the gyroscope in which tumbling exists and inconsistent results were obtained. Tilt-angle variation was from  $0^\circ$  to  $90^\circ$  in  $10^\circ$  increments. Both the angle of bank and yaw were varied from  $0^\circ$  to  $50^\circ$  in  $10^\circ$  increments for each angle of tilt or cant. The pick-off rotation

CONFIDENTIAL

was read visually by means of a pointer mounted on the forward portion of the outer gimbal and a quadrant mounted on the inside of the forward end of the gyro case. The gyroscope was caged momentarily before reading each point to minimize the effect of precession on the validity of the results.

### RESULTS

A comparison between the experimental and calculated response of the gyroscope is presented in figures 15 to 19. These results show the response of the gyro to bank and yaw for various angles of cant and tilt and show that the agreement between experimental and calculated values was very good.

It can be seen that the gyroscope became more sensitive to yaw as the cant angle was decreased (fig. 15) and as the tilt angle was increased (fig. 16). The results in these figures also show that the response of the gyroscope to yaw varied as formula (2) indicates for various cant angles and as formula (3) indicates for various tilt angles. The data of figure 17 show that the response varied linearly with angle of bank over the range of cant angles and figure 18 shows that the gyroscope became more sensitive to bank as the tilt angle was decreased. The results of these figures also show that the response of the gyroscope to bank was constant with cant-angle variation as shown by formula (6) and varied as formula (5) indicates for various tilt angles.

Presented in figure 19 are some representative curves showing the comparison between calculated and experimental results when the cant and tilt angles were varied simultaneously. The results indicate that the response of the gyroscope to yaw varied as formula (1) and the response of the gyroscope to bank as formula (4).

### APPLICATION OF RESULTS

To illustrate the use of formulas (1) and (4) consider, for example, a guided missile which is approaching a target with a glide-path angle of  $30^\circ$  and an angle of attack of  $3^\circ$  with the cant and tilt angles set at  $90^\circ$  and  $80^\circ$ , respectively. Assuming angles of yaw and bank of  $10^\circ$ , the response obtained from angle of yaw (formula (1)) is  $9.8^\circ$  and from the angle of bank (formula (4)) is  $1.6^\circ$ .

If during flight the glide-path angle of the missile changes to  $10^\circ$  with a resultant increase in angle of attack to  $8^\circ$ , there will be changes in cant and tilt angles. This change of  $20^\circ$  in glide-path angle and  $5^\circ$  in angle of attack causes the cant angle to become  $65^\circ$  and the tilt angle  $75^\circ$ . The response from the angle of yaw is now  $10.9^\circ$  for formula (1) and from the angle of bank is  $-1.8^\circ$  for formula (4) for the same angle of yaw and bank. The reversal of response to bank in the final condition would probably cause unstable automatic control.

## REFERENCES

1. Shortal, Joseph A., and Osterhout, Clayton J.: Preliminary Stability and Control Tests in the NACA Free-Flight Wind Tunnel and Correlation with Full-Scale Flight Tests. NACA TN No. 810, 1941.
2. Curfman, Howard J., Jr., and Gardner, William N.: Theoretical Analysis of the Motions of an Aircraft Stabilized in Roll by a Displacement-Response, Flicker-Type Automatic Pilot. NACA RM No. L8D19, 1948.
3. Eshbach, Ovid W., ed.: Handbook of Engineering Fundamentals. John Wiley & Sons, Inc., 1936, pp. 2-27.



TABLE I

## MASS AND AERODYNAMIC CHARACTERISTICS OF FULL-SCALE MISSILE

REPRESENTED BY  $\frac{1}{3}$ -SCALE MODEL TESTED IN LANGLEY FREE-FLIGHT TUNNEL

Weight, W, lb . . . . .	224.5
Wing area S, ft <sup>2</sup> . . . . .	18.07
Wing loading W/S, lb/ft <sup>2</sup> . . . . .	12.43
Relative density factor $\mu$ , m/ $\rho S b$ . . . . .	19.10
Radius of gyration in roll, ft . . . . .	1.09
Radius of gyration in yaw, ft . . . . .	2.668
<sup>1</sup> Directional-stability parameter $C_{n\beta}$ . . . . .	0.00075
<sup>1</sup> Effective-dihedral parameter $C_{l\beta}$ . . . . .	-0.0020
<sup>1</sup> Lateral-force parameter $C_{Y\beta}$ . . . . .	-0.0082
<sup>2</sup> Damping in roll $L_{\dot{\phi}}$ . . . . .	0.0779
<sup>2</sup> Rolling moments caused by full control deflection $\delta_{aL}\delta_a$ . . . . .	1.89

<sup>1</sup>From force tests of the model.<sup>2</sup>Used in calculation of rolling motion of model.

TABLE II

TABLE OF TEST CONDITIONS

Test	Type of control	Rudder deflection (deg)	Aileron deflection (deg)	Cent angle (deg)	Transition angle (deg)	Control neutralizing springs	Figure
1	Hunting	$\pm 7$	$\pm 25$	22.5	10	On	10
2	---do---	$\pm 7$	$\pm 25$	90.0	10	On	10
3	---do---	$\pm 7$	$\pm 25$	45.0	10	On	9,10,11
4	---do---	0	$\pm 25$	45.0	10	On	11
5	---do---	$\pm 7$	$\pm 25$	45.0	5	On	9
6	Flicker	$\pm 7$	$\pm 25$	45.0	0	On	9,12,13
7	---do---	$\pm 7$	$\pm 25$	45.0	0	Off	12



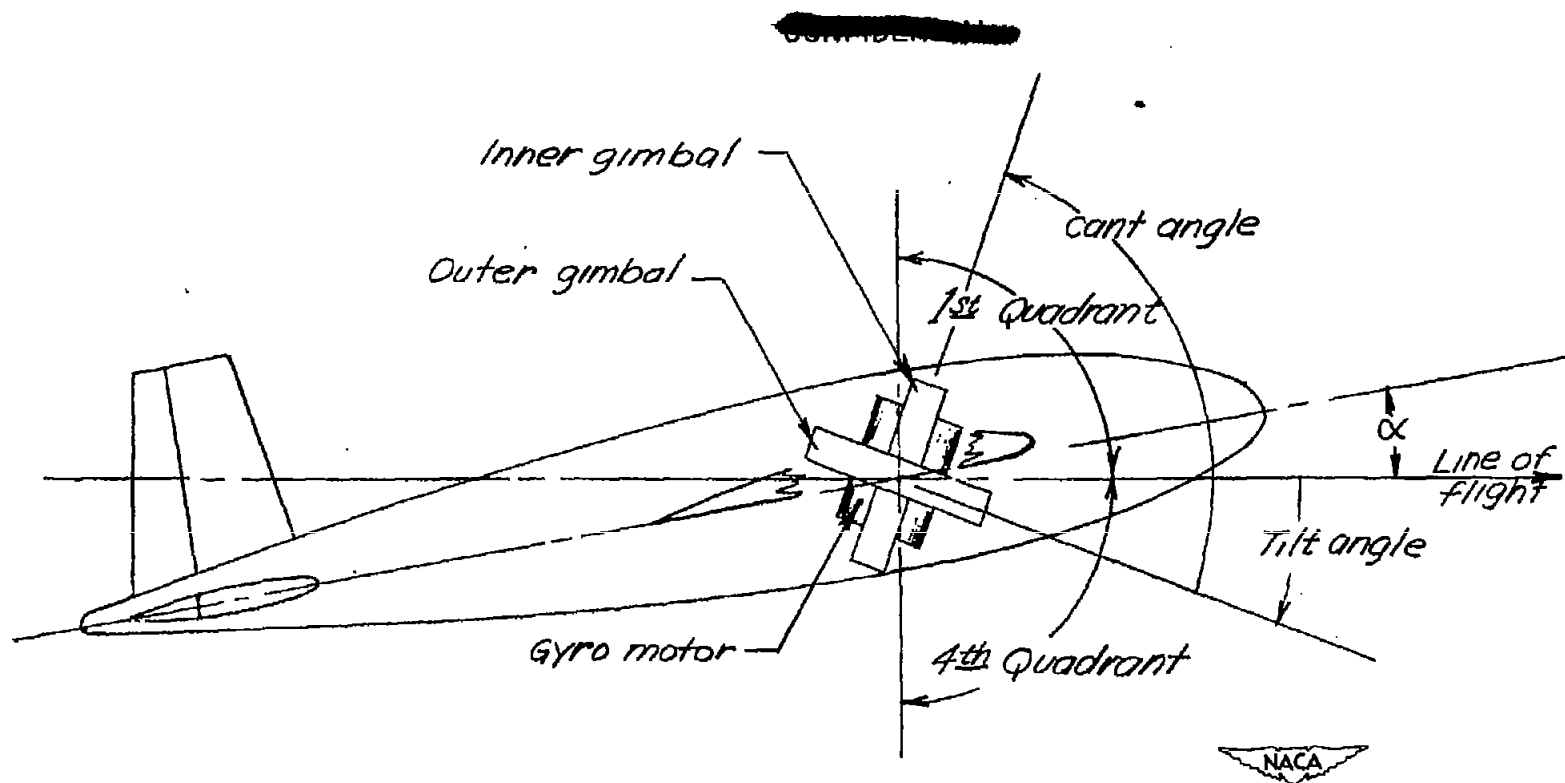


Figure 1.- Definition of cant and tilt angles. Arrows indicate positive directions.

[REDACTED]

[REDACTED]

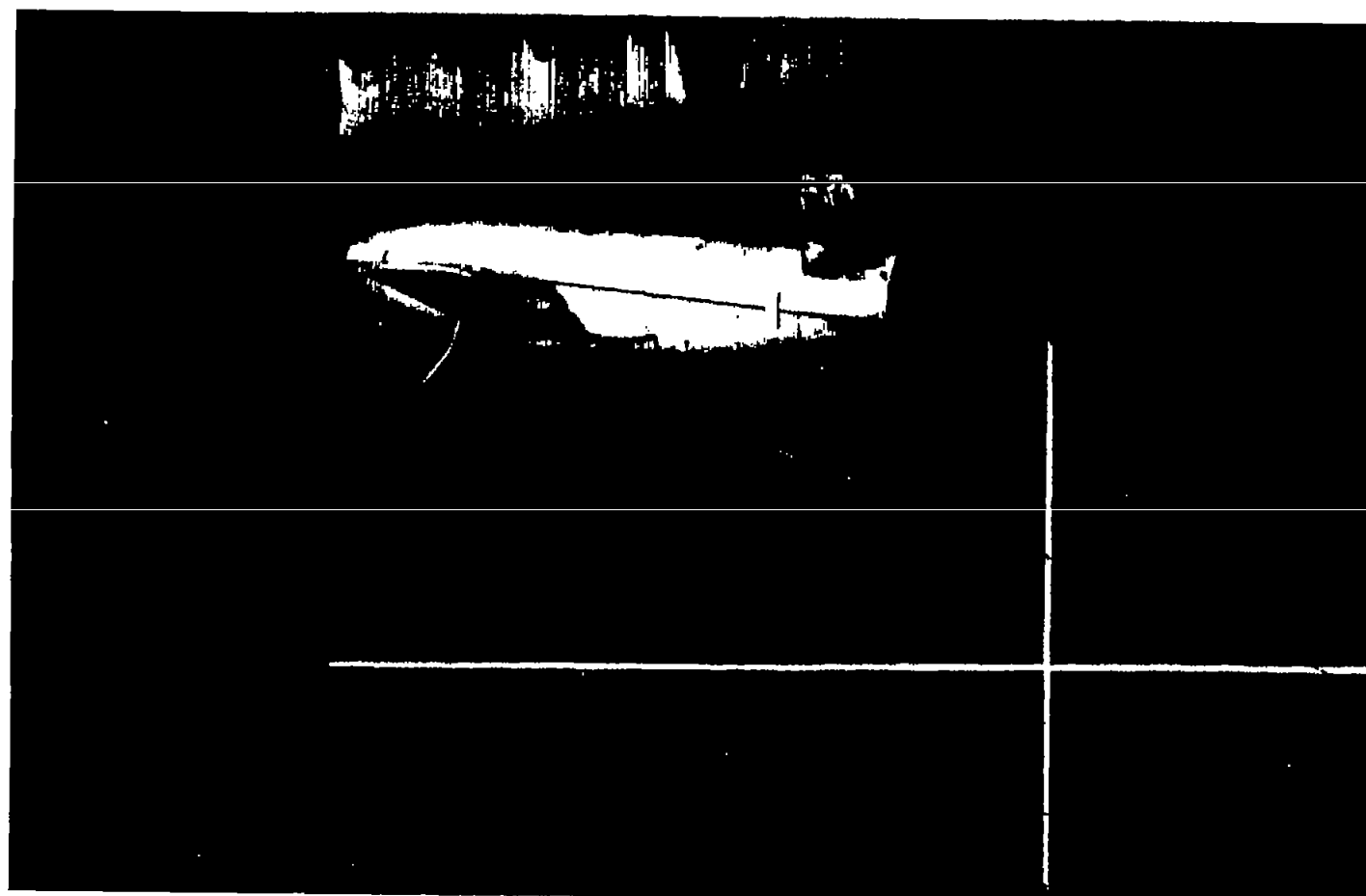


Figure 2.- Test section of Langley free-flight tunnel showing model in flight.

NACA  
L-42261



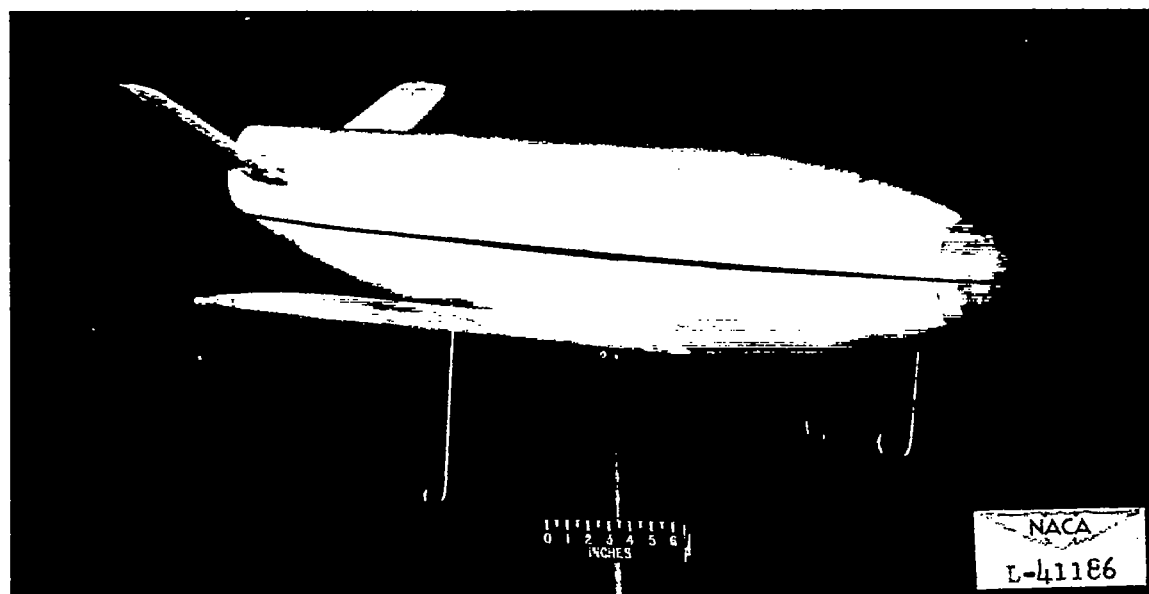
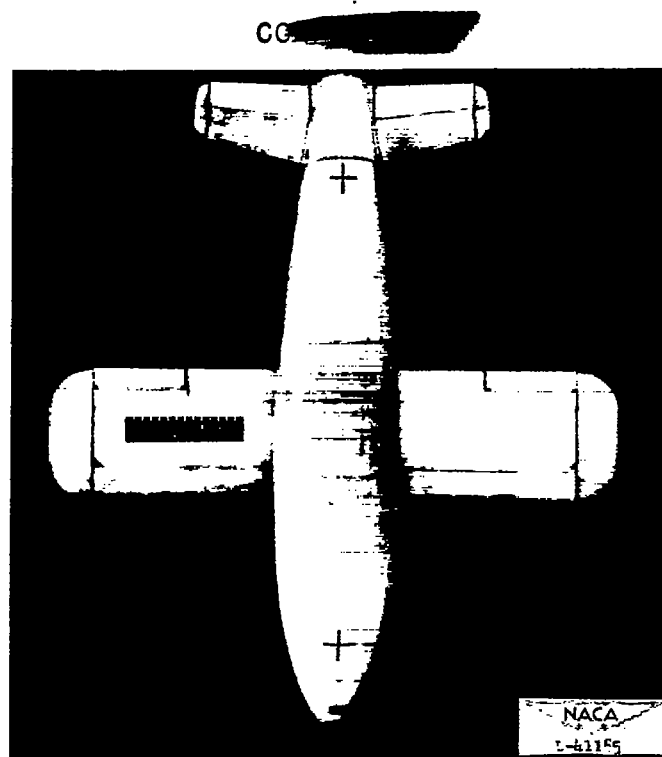


Figure 3.- One-third scale model used in the Langley free-flight-tunnel investigation.

100

100

100

100

100

100

100

100

100

100

100

100

100

100

100

100

100

100

100

100



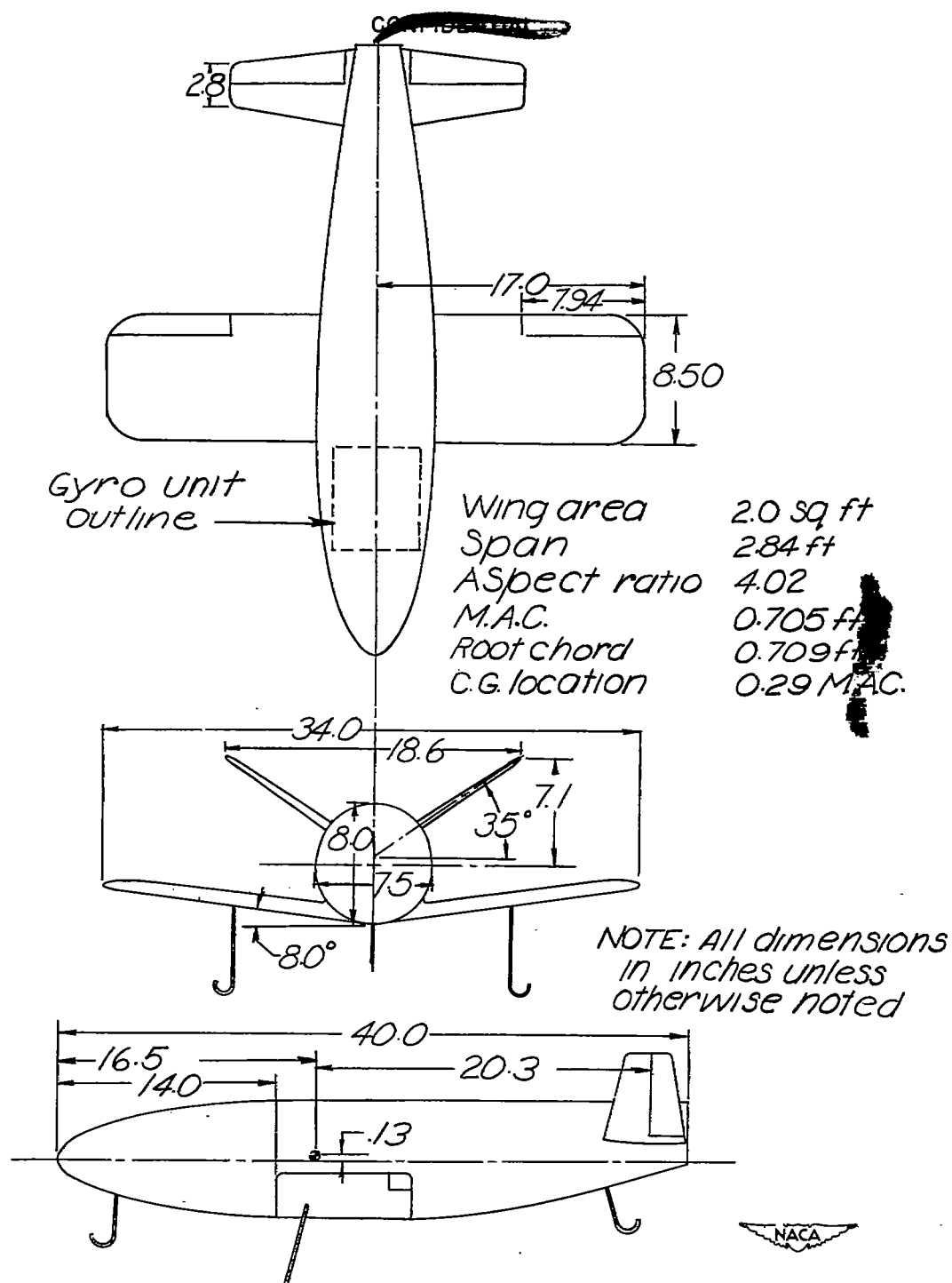
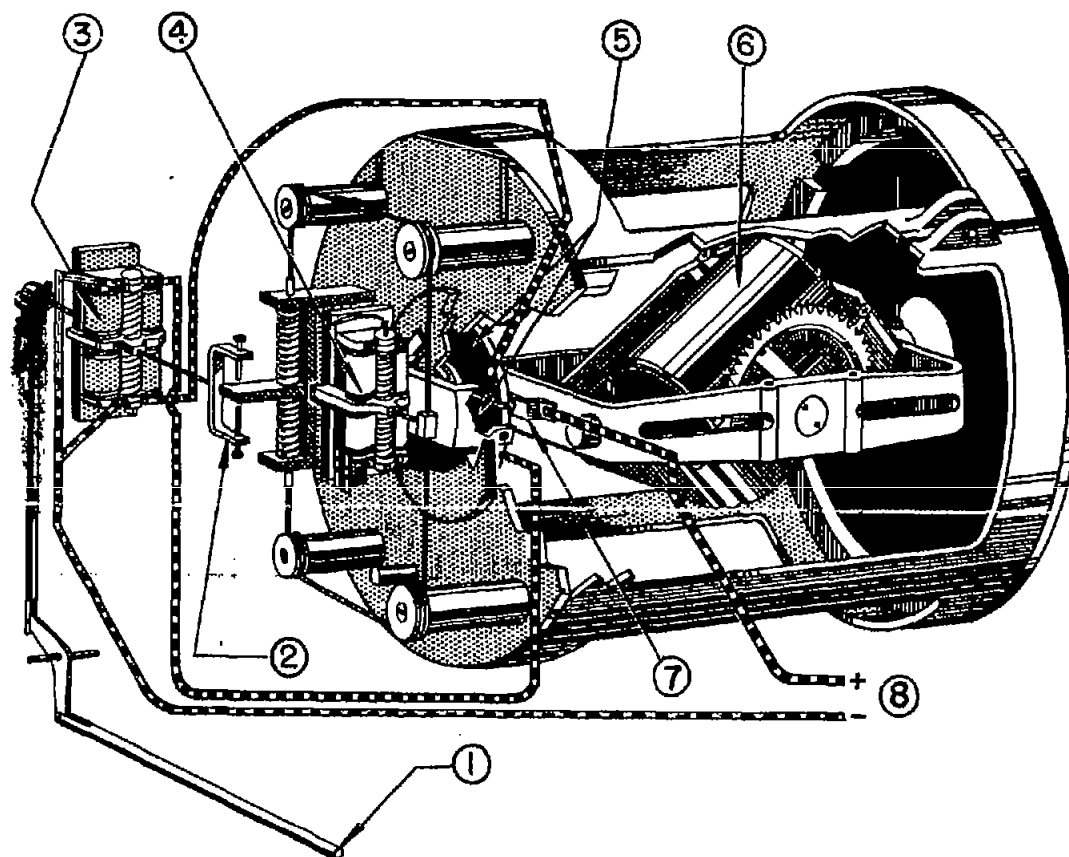


Figure 4.- Three-view sketch of model used in the Langley free-flight-tunnel investigation.

CONFIDENTIAL



- 1 - To controls
- 2 - Reversing attachment  
(installed only for hunting  
control)
- 3 - Control actuating mechanism
- 4 - Pilot's override mechanism  
(mounted on pick-off drum)
- 5 - Left and right segments of  
pick-off drum
- 6 - Gyro motor
- 7 - Pick-off contact (mounted  
on outside gimbal)
- 8 - Power source



Figure 5.- Sketch of gyro unit showing location of component parts.

CONFIDENTIAL

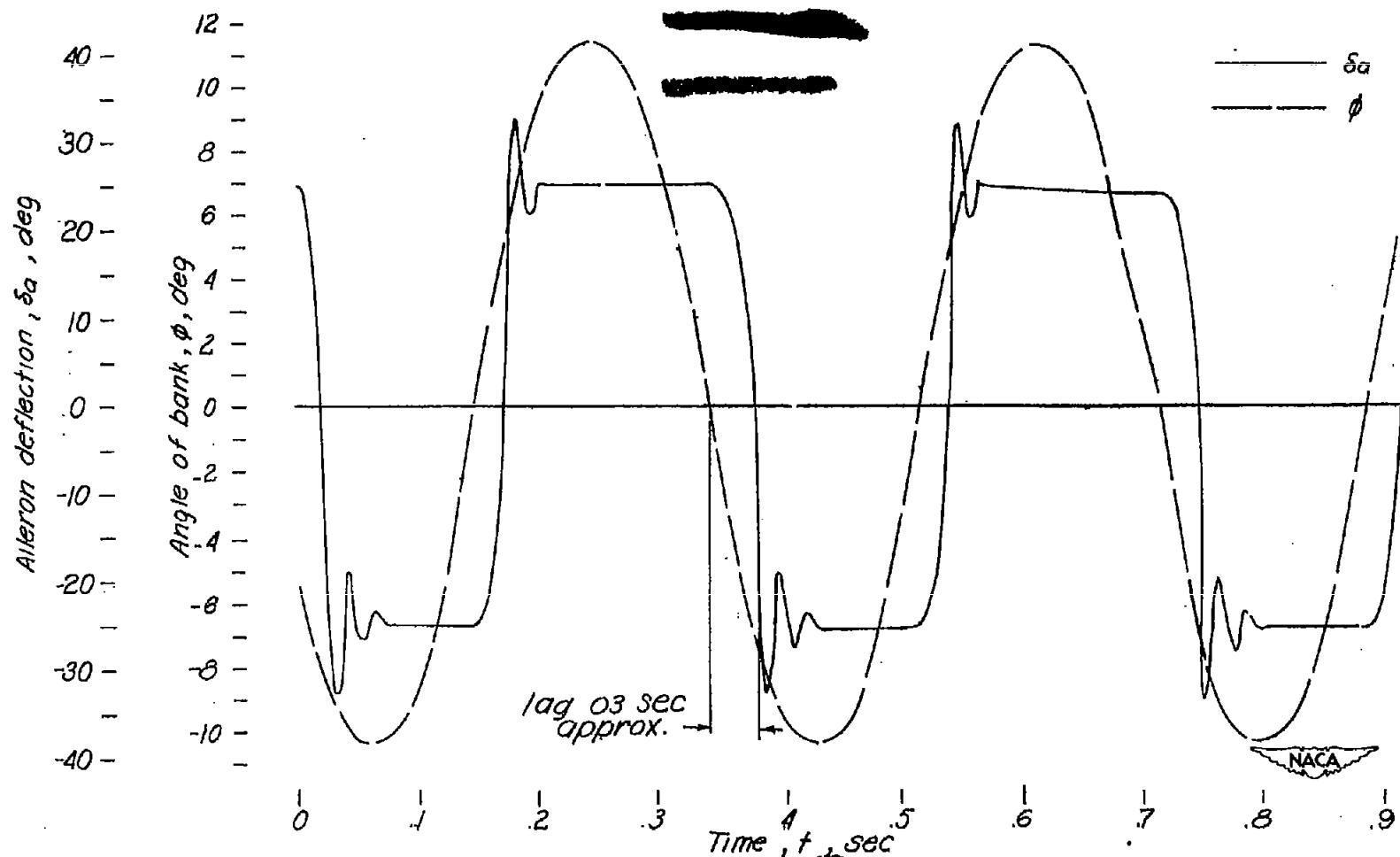


Figure 6.- Illustration of flicker control as obtained from oscillating-table tests.

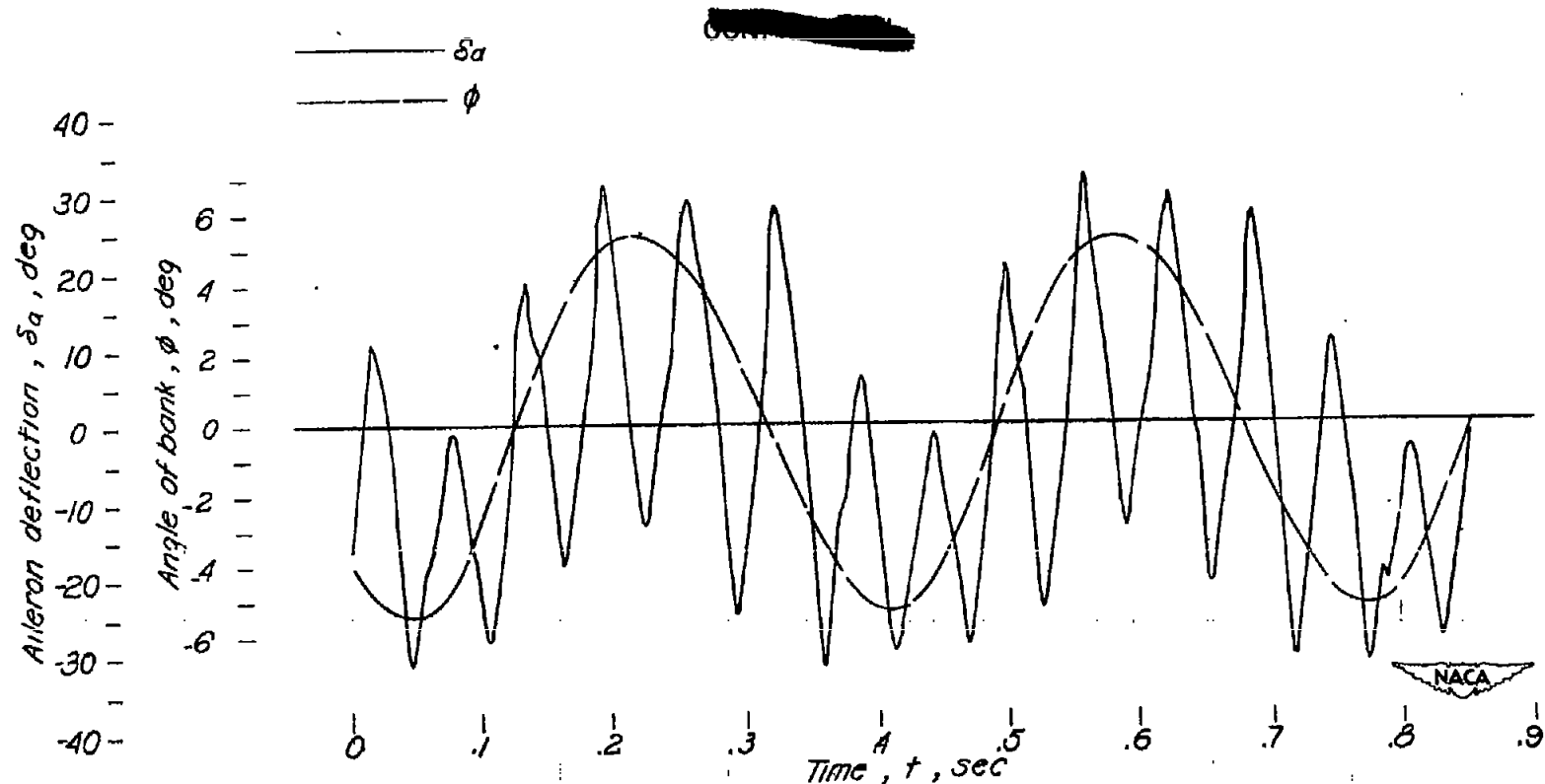


Figure 7.- Illustration of hunting control as obtained from oscillating-table tests with transition angle larger than maximum angle of roll.

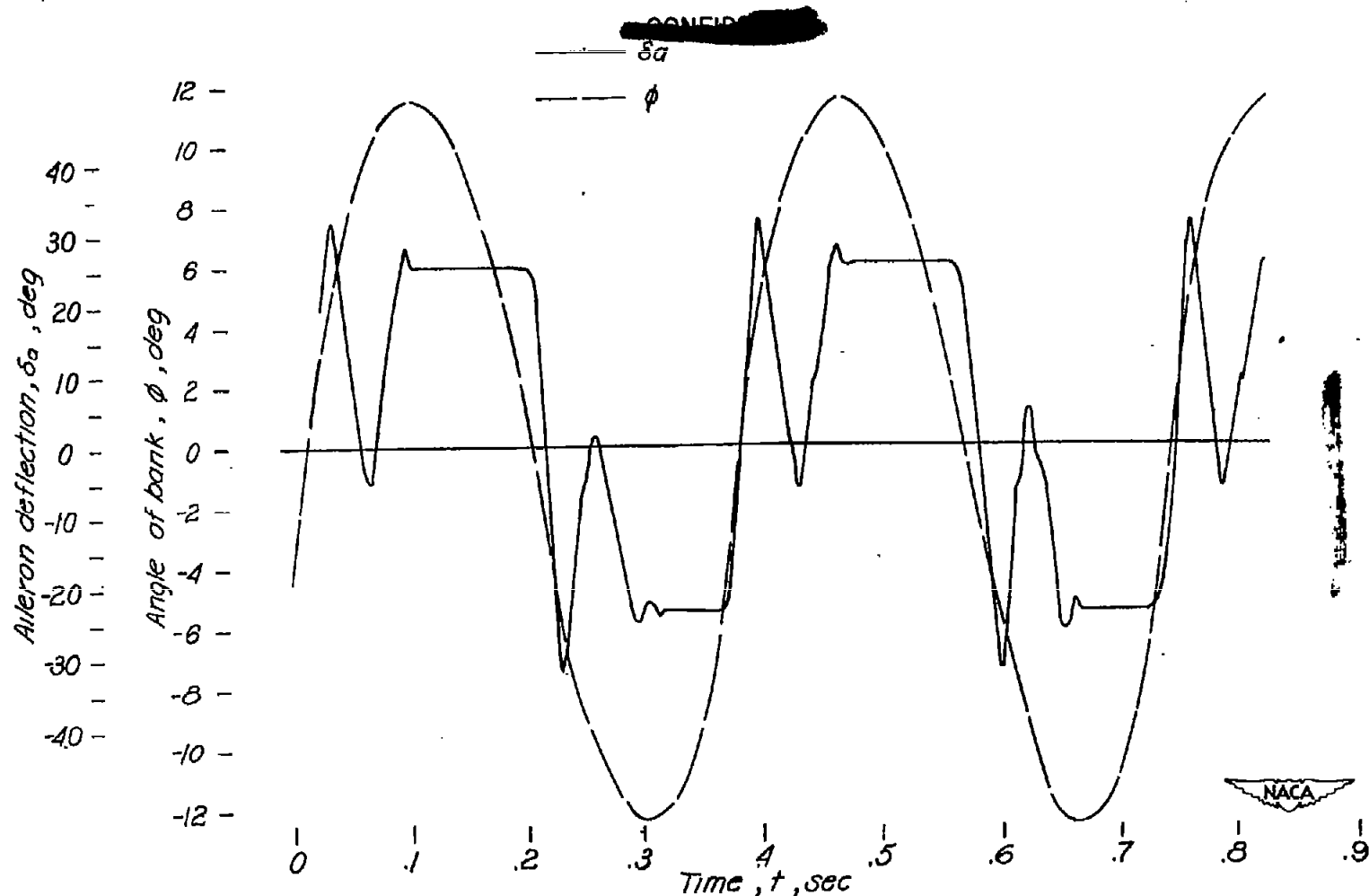


Figure 8.- Illustration of hunting control as obtained from oscillating-table tests with transition angle less than maximum angle of roll.

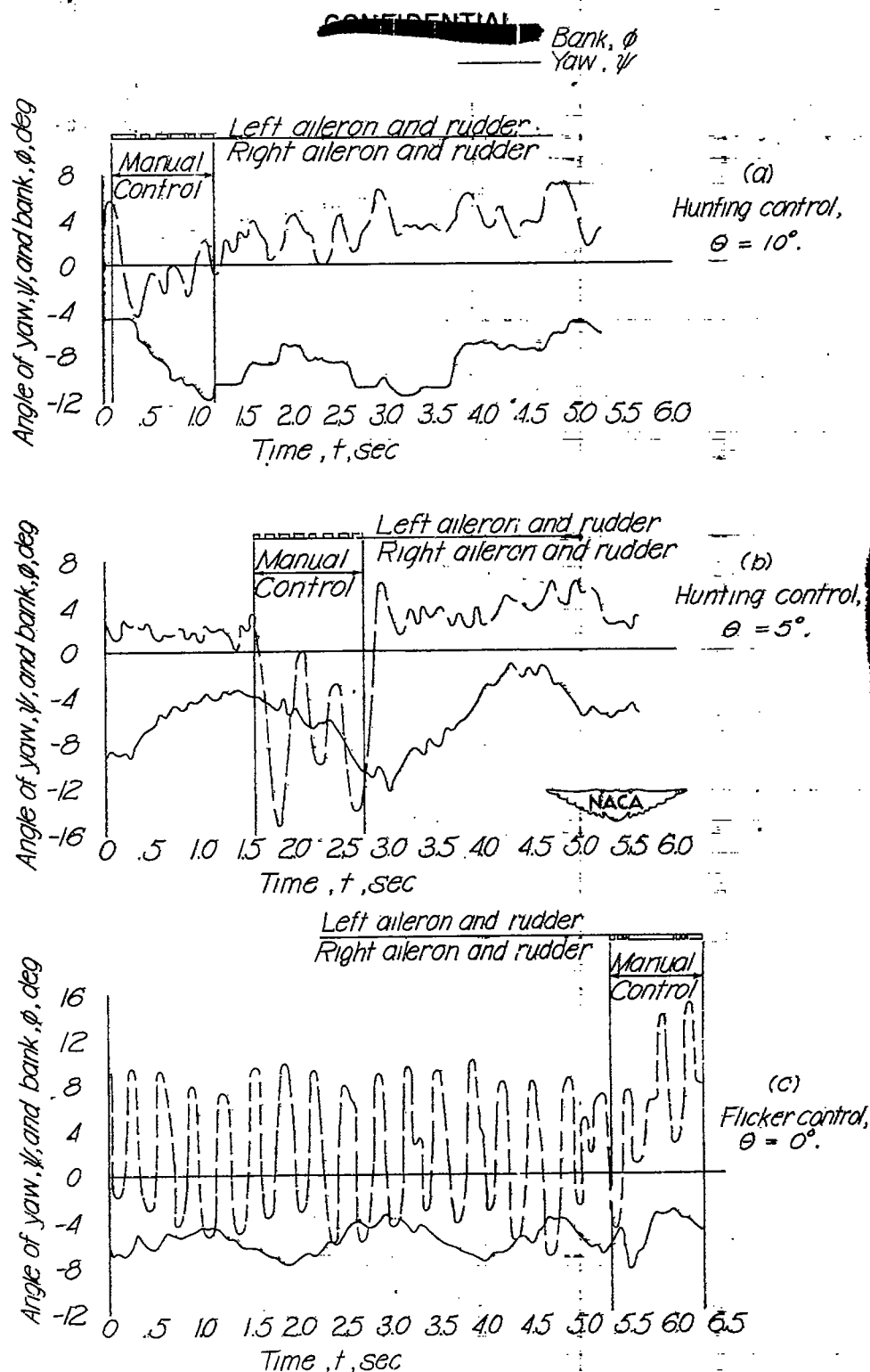


Figure 9.- Typical flight records of lateral motions of the model showing the effect of varying type of control. Cant angle,  $45^\circ$ ;  $\delta_a = \pm 25^\circ$ ;  $\delta_r = \pm 7^\circ$ .

~~CONFIDENTIAL~~

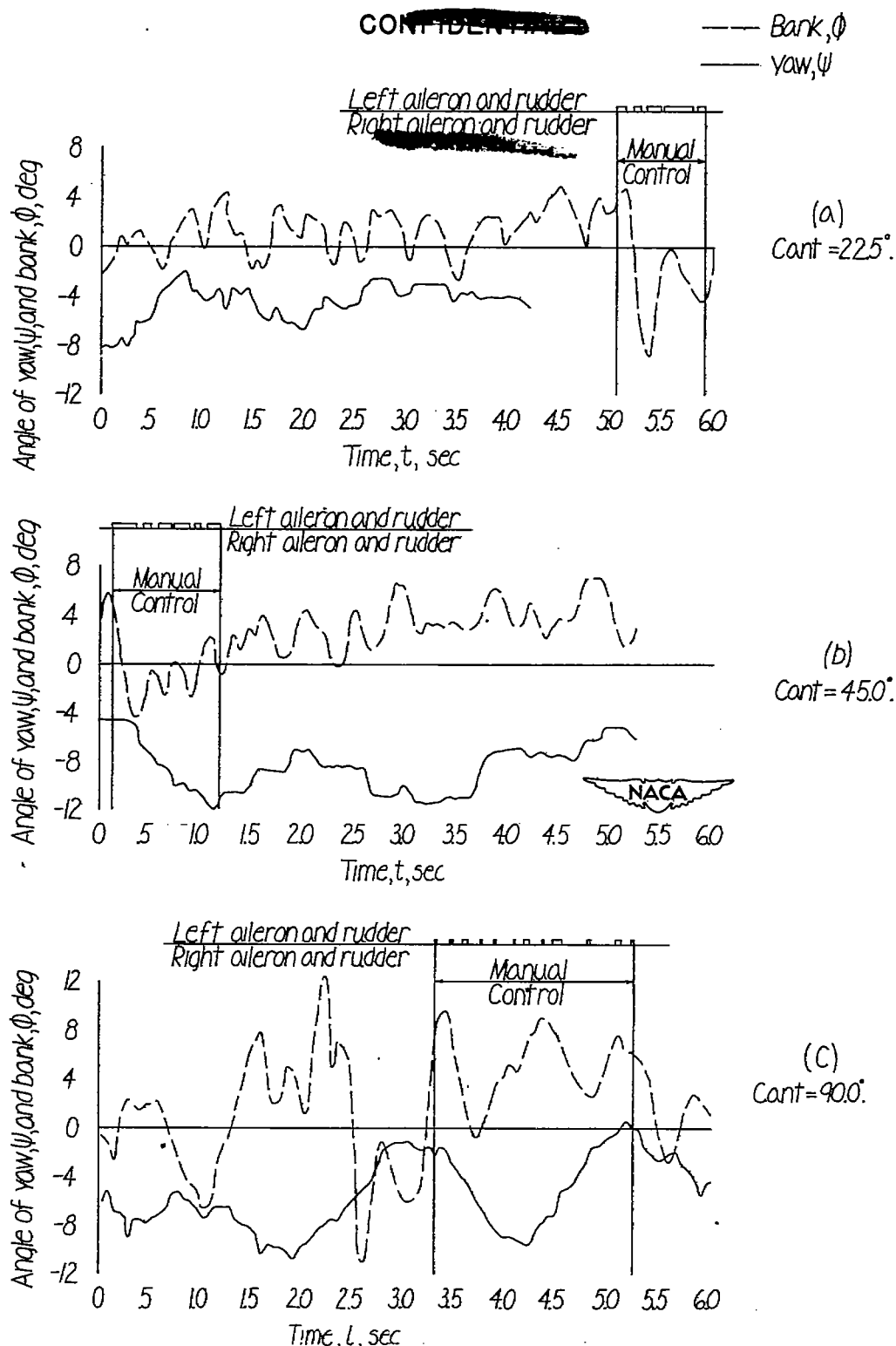


Figure 10.- Typical flight records of lateral motions of the model showing the effect of varying cant angle.  $\theta = 10^\circ$ ;  $\delta_a = \pm 25^\circ$ ;  $\delta_r = \pm 7^\circ$ .

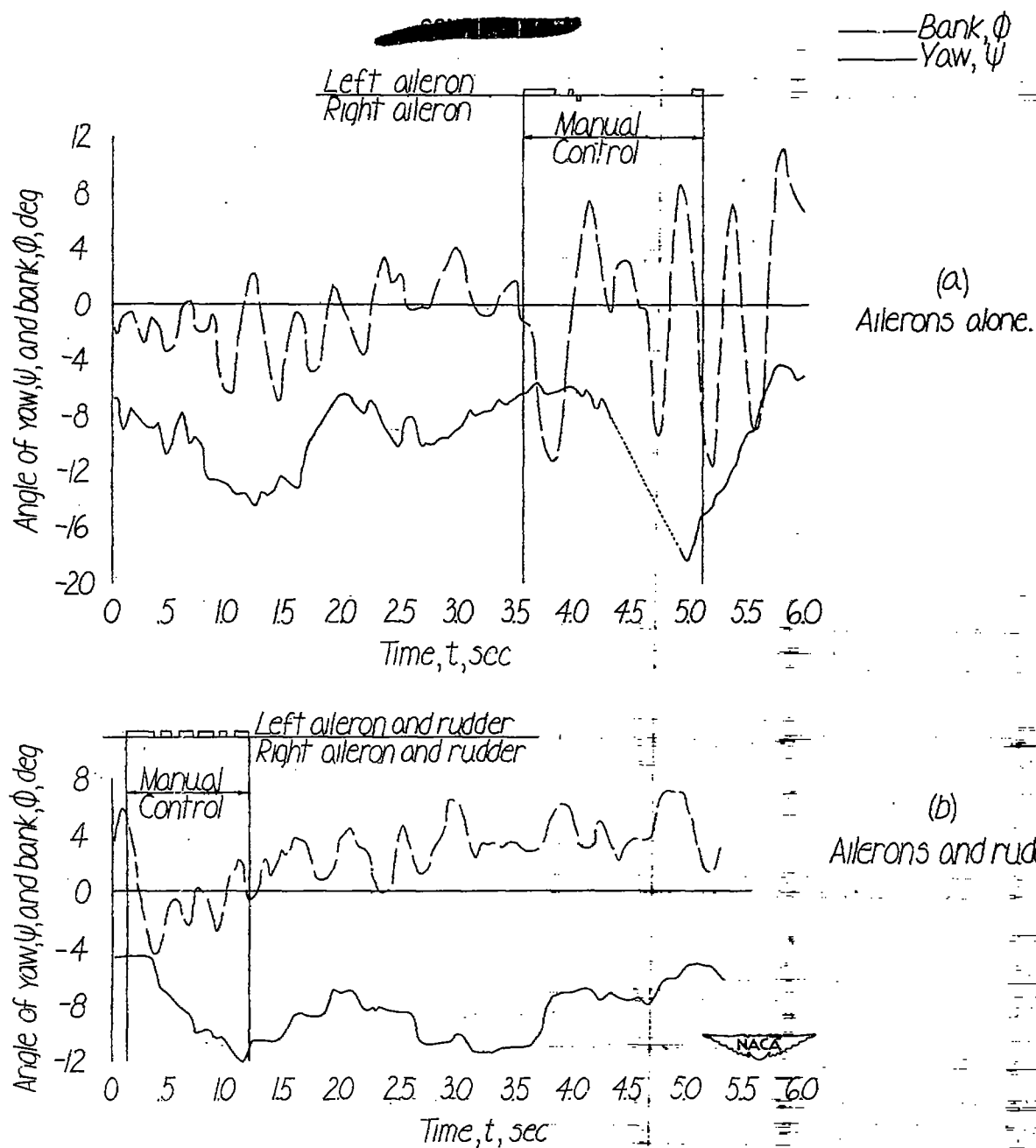


Figure 11.- Typical flight records of lateral motions of the model showing the effect of rudder operation.  $\theta = 10^\circ$ ; cant angle,  $45^\circ$ ;  $\delta_a = \pm 25^\circ$ .



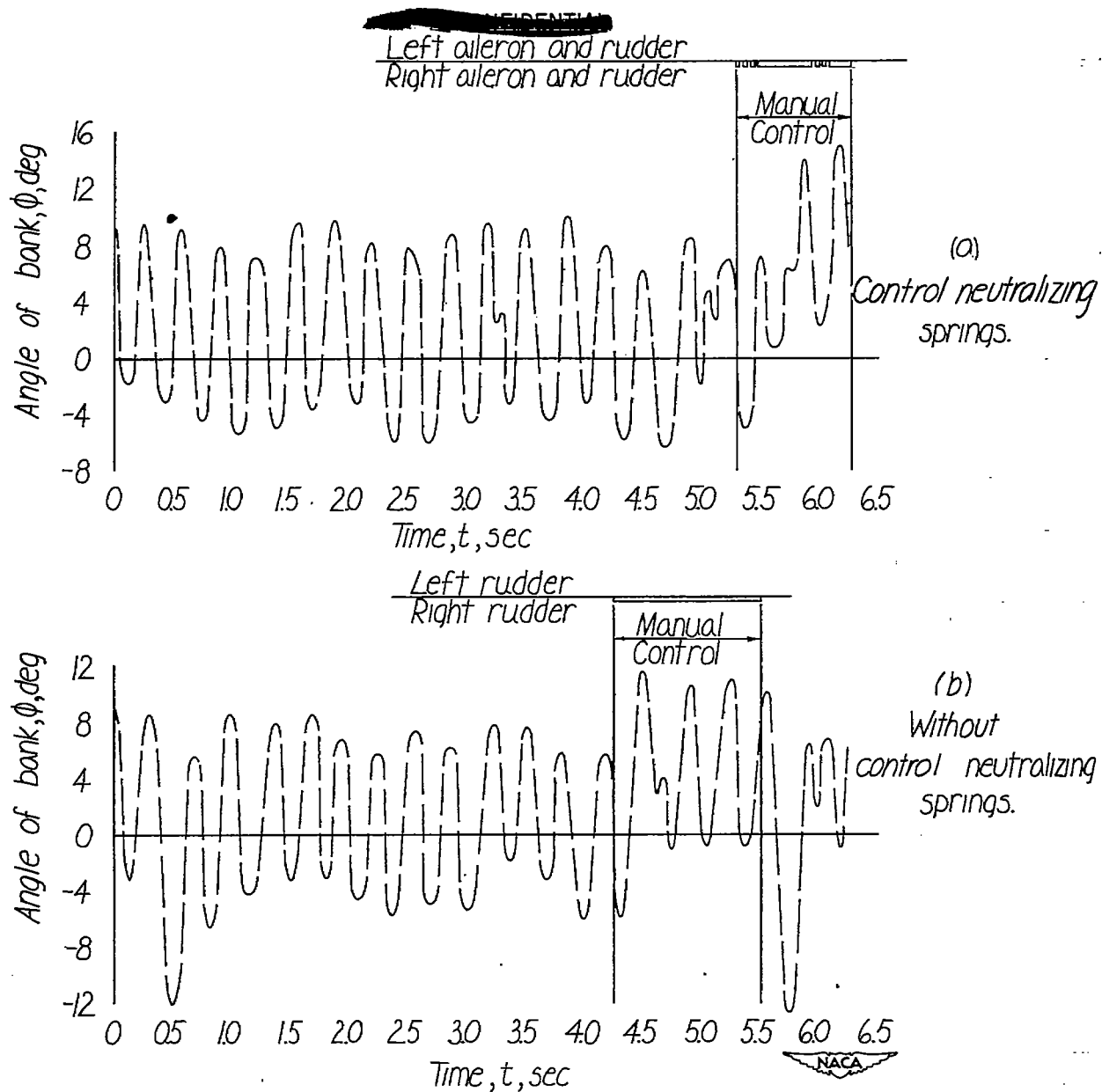


Figure 12.- Typical flight records of lateral motions of the model showing effect of control neutralizing springs.  $\theta = 0^\circ$ ; cant angle,  $45^\circ$ ;  $\delta_a = \pm 25^\circ$ ;  $\delta_r = \pm 7^\circ$ .

~~CONFIDENTIAL~~

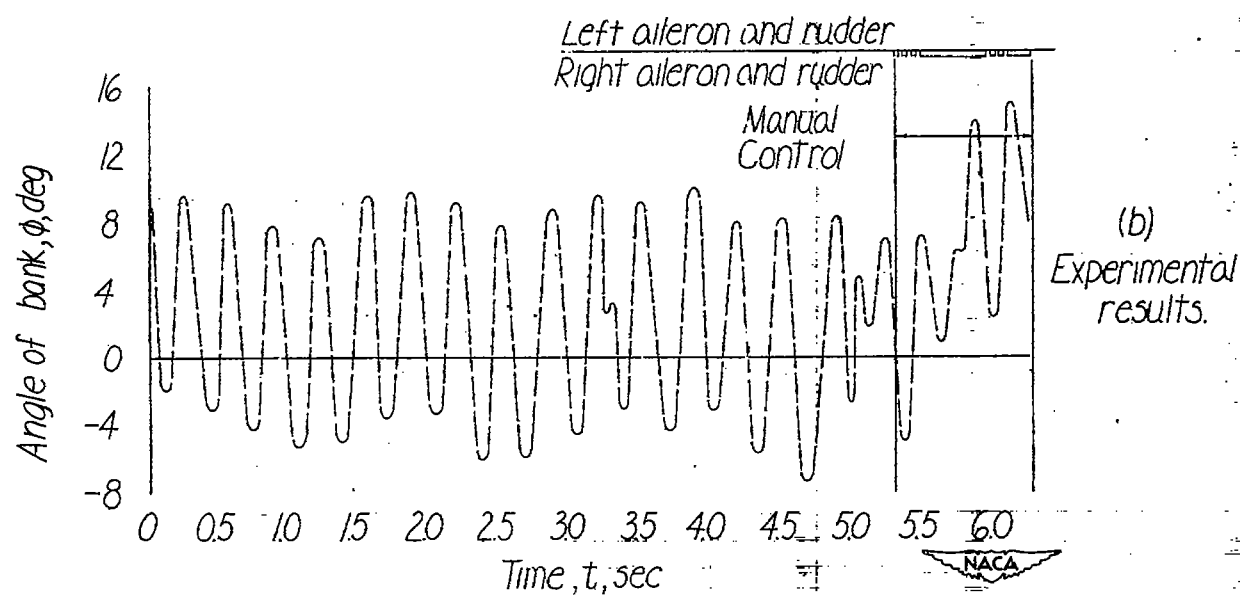
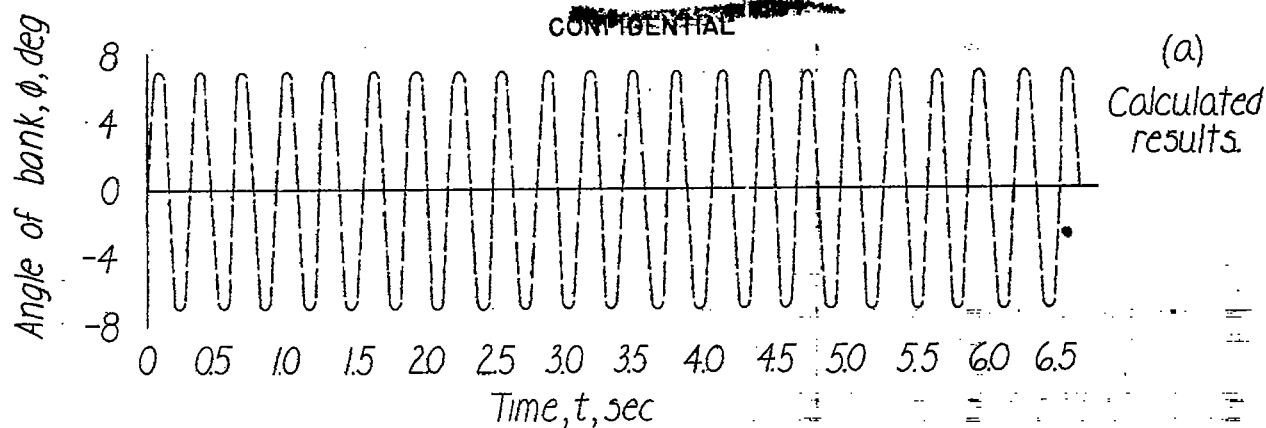


Figure 13.- Comparison of calculated rolling motion with rolling motion obtained from flight records of the model with flicker control.  
 $\theta = 0^\circ$ ; cant angle,  $45^\circ$ ;  $\delta_a = \pm 25^\circ$ ;  $\delta_r = \pm 7^\circ$ .

~~CONFIDENTIAL~~

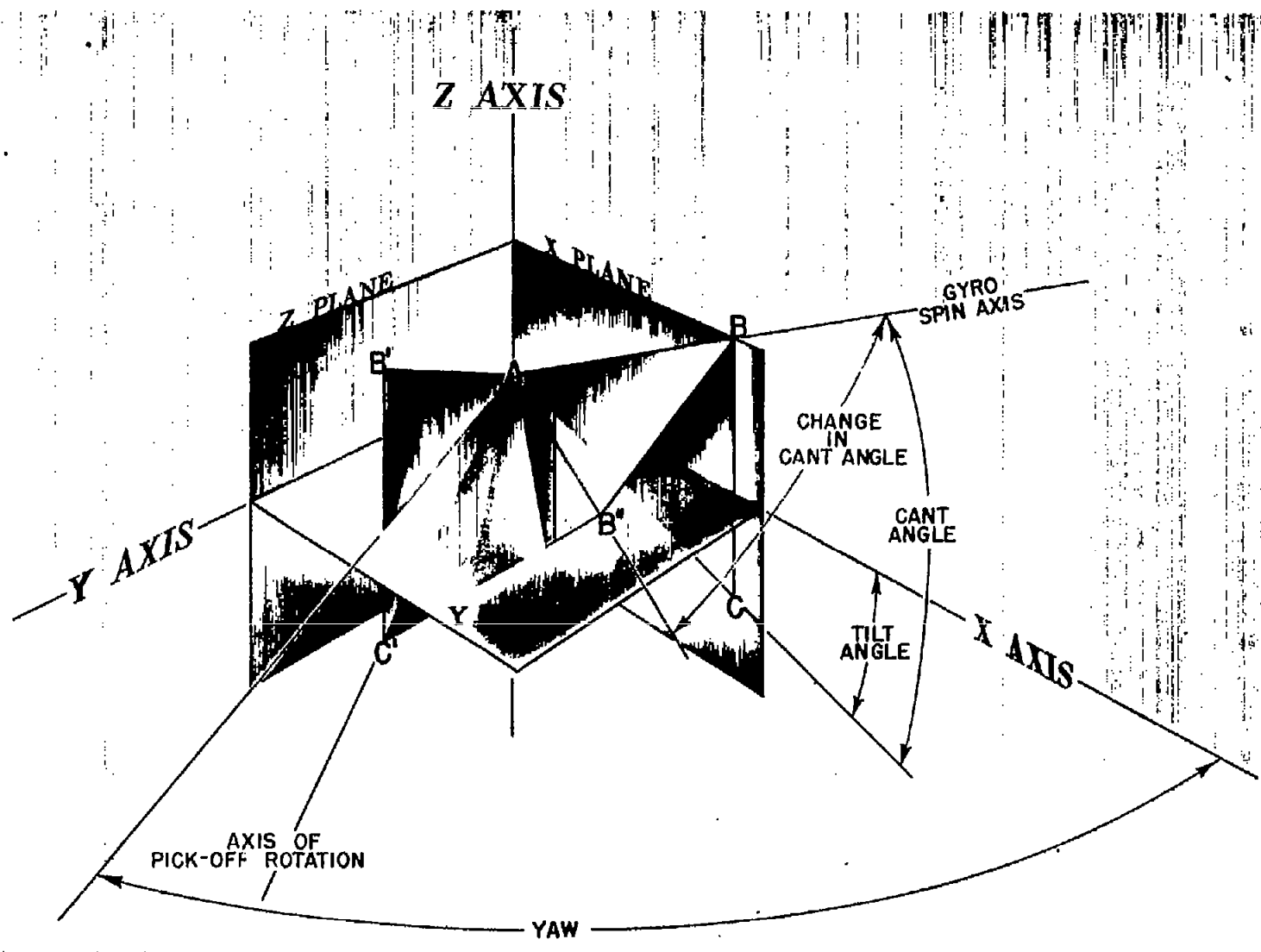


Figure 14.- Relationships used in derivation of formula used in calculating the response of the gyroscope to angle of yaw.



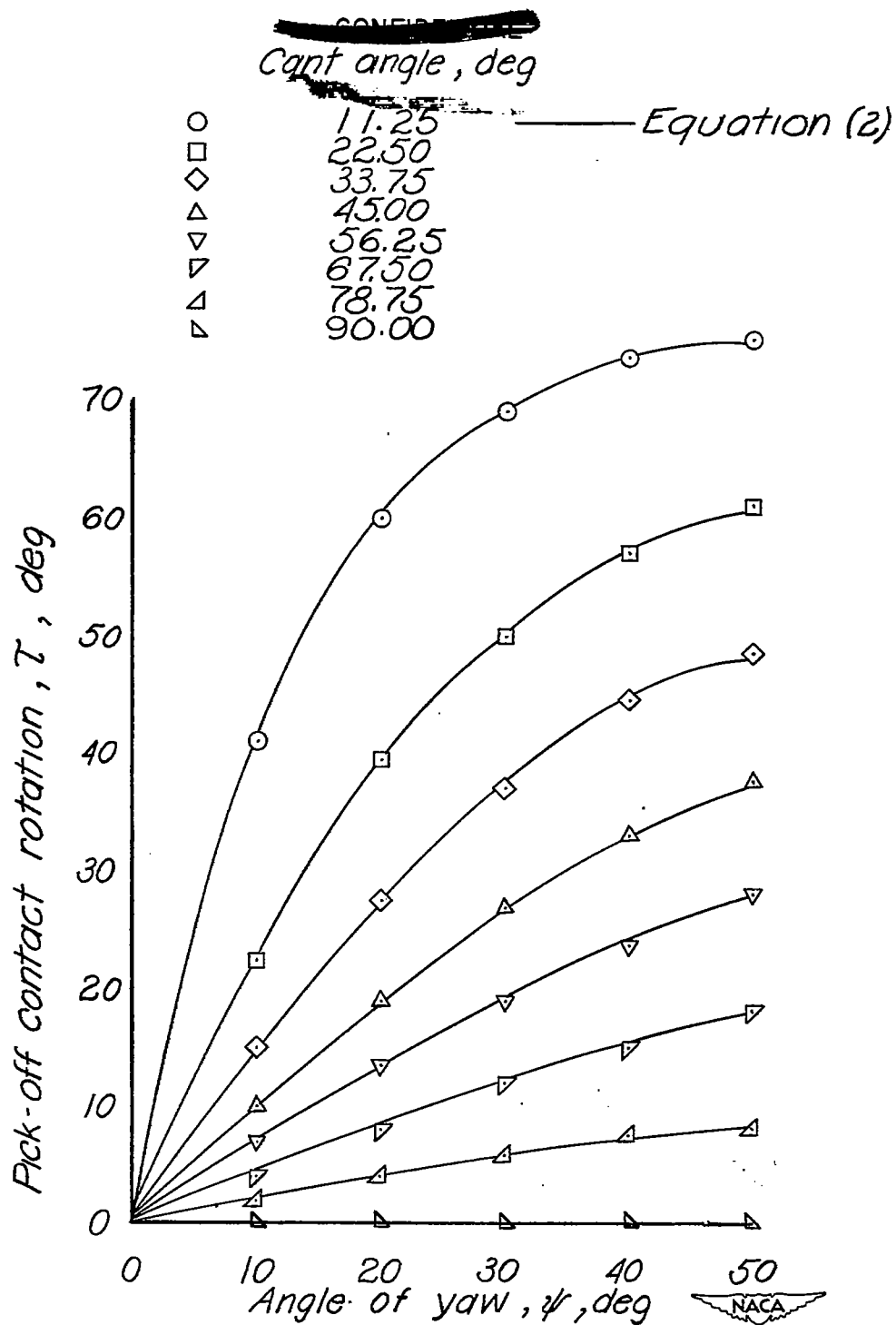


Figure 15.- Comparison of calculated and experimental results of gyro response to yaw over a range of cant angles. Tilt 0°.

~~CONFIDENTIAL~~

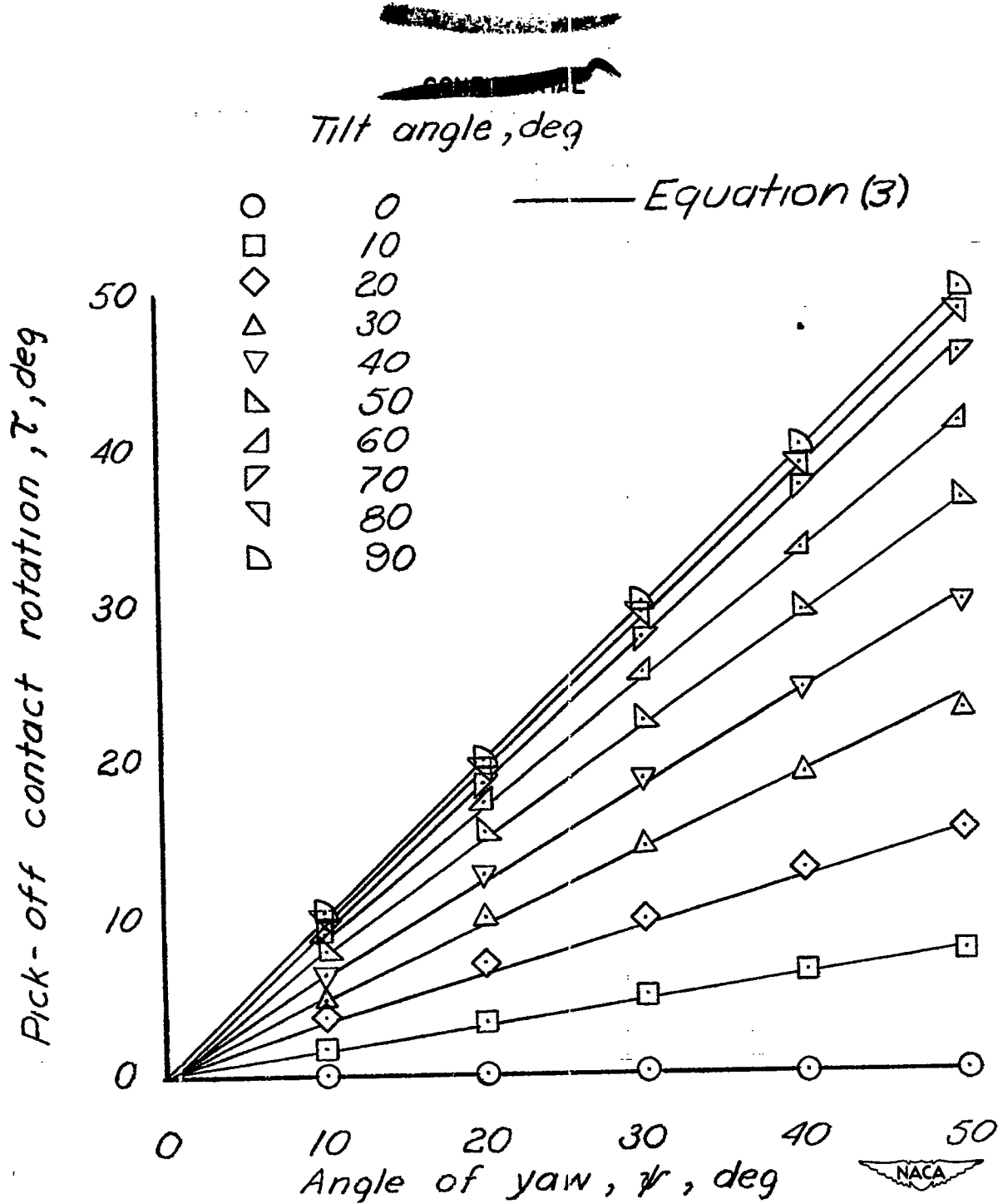


Figure 16.- Comparison of calculated and experimental results of gyro response to yaw over a range of tilt angles. Cant 90°.

~~CONFIDENTIAL~~

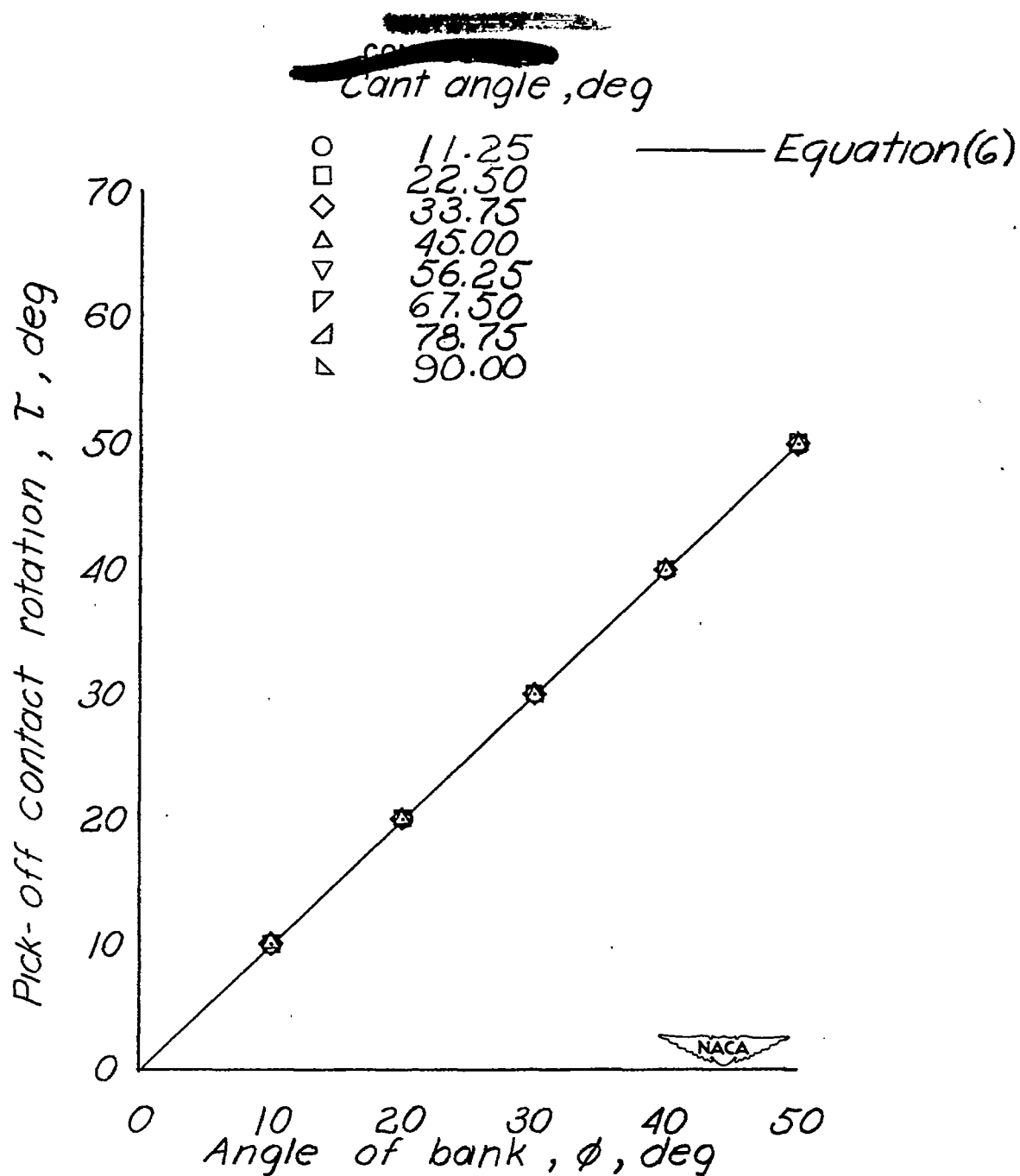


Figure 17.- Comparison of calculated and experimental results of gyro response to bank over a range of cant angles. Tilt 0°.

~~CONFIDENTIAL~~

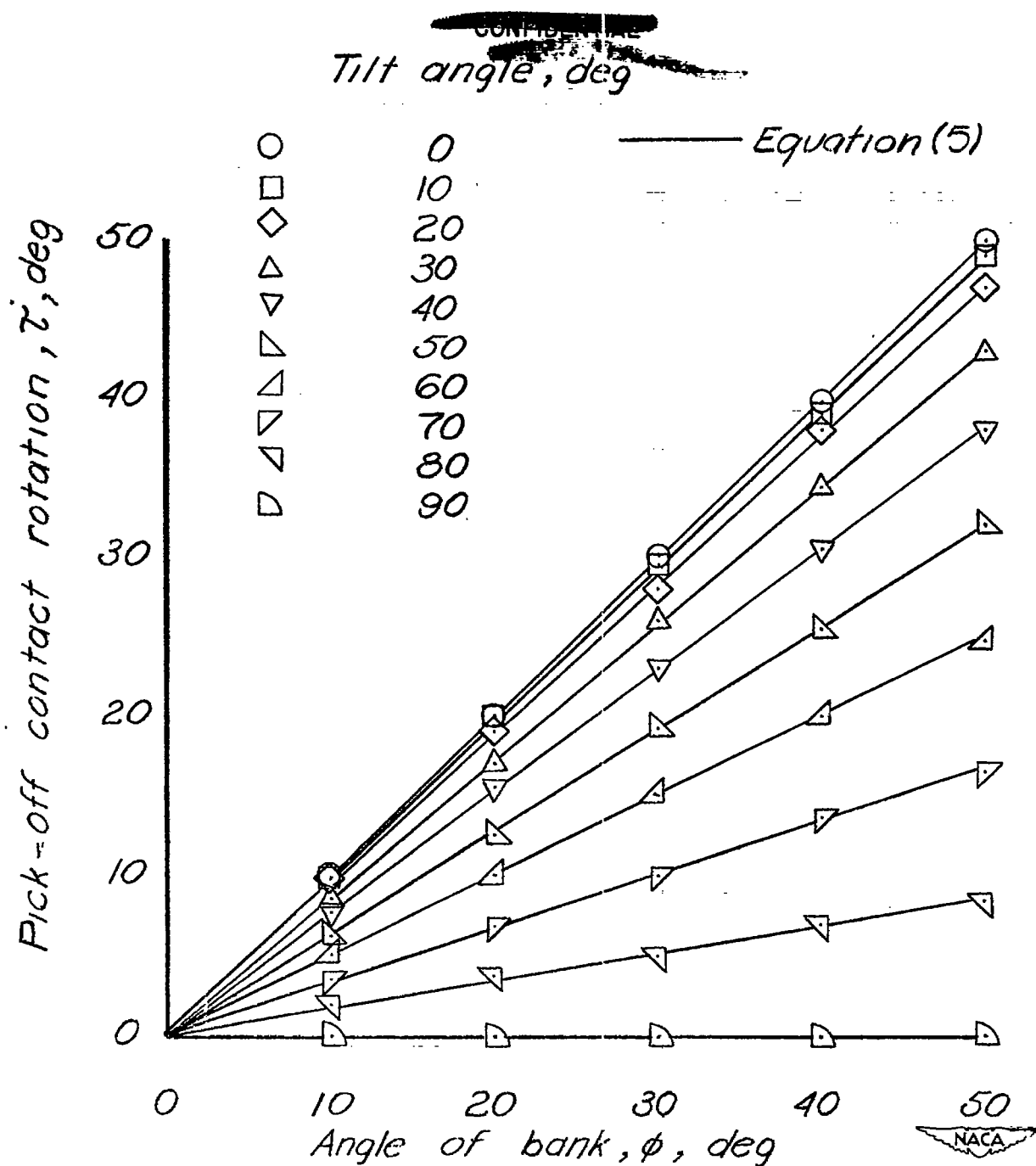


Figure 18.- Comparison of calculated and experimental results of gyro response to bank over a range of tilt angles. Cant 90°.



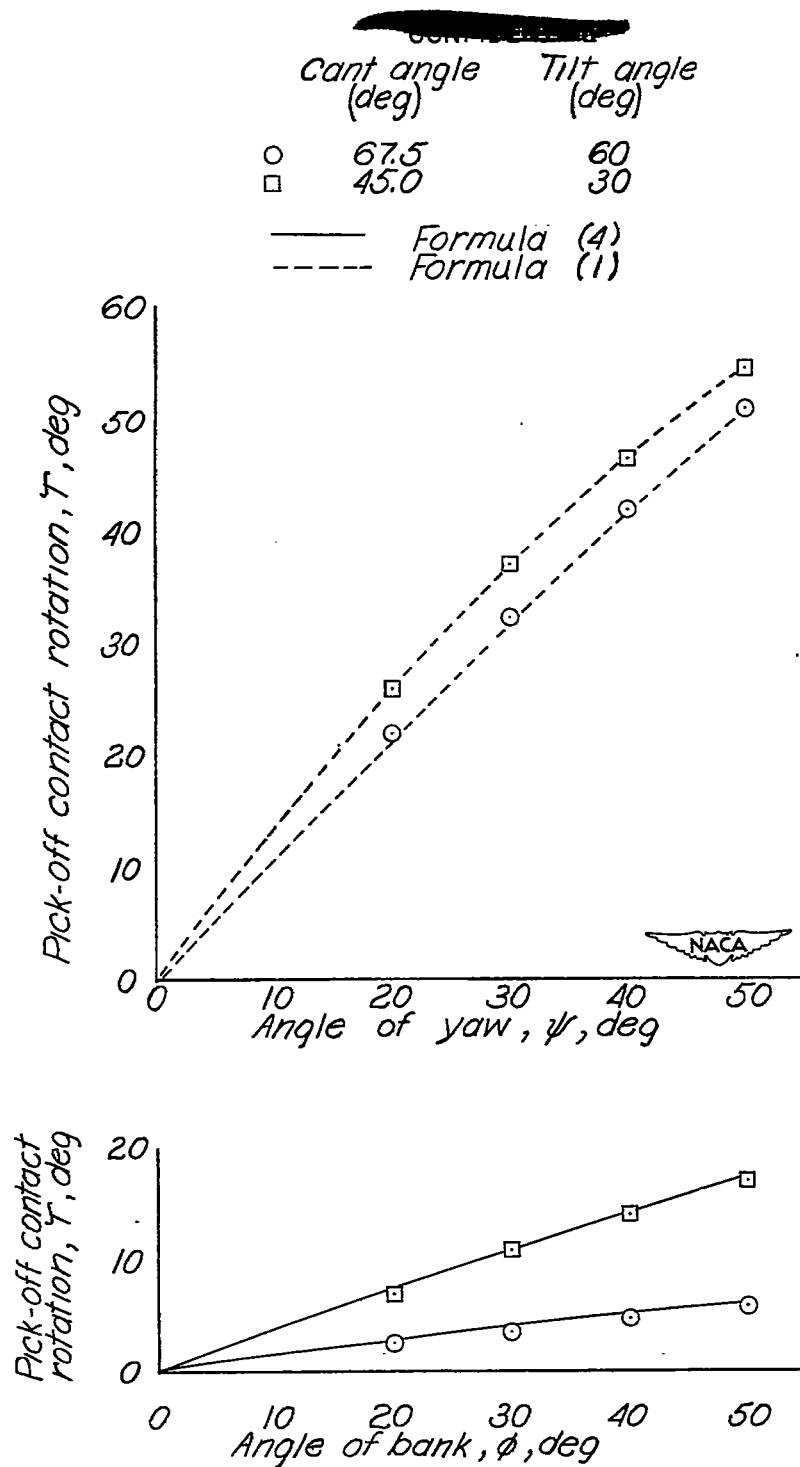


Figure 19.- Comparison of calculated and experimental results of gyro response to bank and yaw with cant and tilt angles varied simultaneously. ~~CONFIDENTIAL~~